An ab Initio Excursion on the Lowest 18 Electronic Surfaces of the NCl + NCl System: Some Insight into the Long-Range Self-Quenching Pathways of the First Excited State of NCl†

Gregory S. Tschumper,*,‡,§ Michael C. Heaven,§ and Keiji Morokuma*,§

Department of Chemistry and Biochemistry, University of Mississippi, University, Mississippi 38677-1848, and Cherry L. Emerson Center for Scientific Computation and Department of Chemistry, Emory University, Atltanta, Georgia 30322

Received: February 26, 2002; In Final Form: May 8, 2002

A series of state-averaged complete active space self-consistent field (SA-CASSCF) computations were carried out in search of low-energy self-annihilation pathways for two NCl molecules in their first excited state ($a^1\Delta$). Numerous scans of the lowest 18 electronic surfaces that correlate with the interaction of two NCl molecules in the $X^3\Sigma^-$, $a^1\Delta$, and $b^1\Sigma^+$ states are reported. Eight long-range, low-energy pathways were located (four in C_{2v} and eight in C_{2h} symmetry) that connect NCl($a^1\Delta$) + NCl($a^1\Delta$) to NCl($X^3\Sigma^-$) + NCl($b^1\Sigma^+$) and NCl($X^3\Sigma^-$) + NCl($a^1\Delta$). It was possible to rigorously characterize the minima on four of these seams of crossings (MSXs). The MSXs between the a + a manifold and the X + b manifold are only 1.8−4.5 kcal mol^{-1} above the a + a asymptote and therefore energetically accessible. Additional scans suggest these MSXs are planar but, to some extent, prefer to distort from C_{2v} cis and C_{2h} trans structures to C_s orientations, which would lower the MSX energies slightly.

Introduction

Like molecular oxygen, the first excited state of NCl ($a^1\Delta$) can chemically drive an iodine laser system.[1−5]

$$O_2(a^1\Delta_g) + I(^2P_{3/2}) \rightleftharpoons O_2(X^3\Sigma_g^-) + I(^2P_{1/2}) \quad (1)$$

$$NCl(a^1\Delta) + I(^2P_{3/2}) \rightleftharpoons NCl(X^3\Sigma^-) + I(^2P_{1/2}) \quad (2)$$

The former is referred to as a chemical oxygen/iodine laser (COIL) system, while the latter is often called a chemical azide/iodine laser (CAIL) system (since azide is used in the process which generates the excited NCl[6]). The first CAIL device was demonstrated by Henshaw et al.[7] CAIL efficiency clearly depends on the concentration of the energy carrier NCl($a^1\Delta$). Unfortunately, a high concentration of this metastable species will cause some self-annihilation. For example

$$NCl(a^1\Delta) + NCl(a^1\Delta) \rightleftharpoons NCl(X^3\Sigma^-) + NCl(b^1\Sigma^+) \quad (3)$$

$$\rightleftharpoons NCl(X^3\Sigma^-) + NCl(a^1\Delta) + E_{trans,vib} \quad (4)$$

$$\rightleftharpoons NCl(X^3\Sigma^-) + NCl(X^3\Sigma^-) + E_{trans,vib} \quad (5)$$

Setser has made important contributions to understanding the rate constants of processes that generate and quench NCl($a^1\Delta$).[8−10] However, relatively few reactions have been characterized to date. At present it is not possible to predict the conditions that will maximize generation of excited I($^2P_{1/2}$) by NCl(a) pumping, as our knowledge of NCl(a) energy transfer and reaction kinetics is not adequate. In particular, the self-quenching of NCl($a^1\Delta$) is an important energy loss mechanism about which many aspects are unknown. In addition, much of what is known consists of rate constants obtained at room temperature while CAIL systems will operate at temperatures near 600 K.

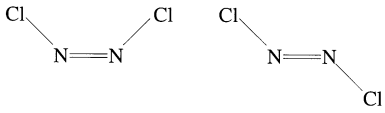

Figure 1. C_{2v} structure of the cis isomer and C_{2h} structure of the trans isomer of dichlorodiazene.

The spectroscopic properties of NCl are well-known from both experimental and theoretical studies. Two metastable excited states ($a^1\Delta$ and $b^1\Sigma^+$) exist in addition to the ground state ($X^3\Sigma^-$), all of which possess the following electronic configuration: $1\sigma^2\ 2\sigma^2\ 3\sigma^2\ 4\sigma^2\ 1\pi^4\ 5\sigma^2\ 6\sigma^2\ 7\sigma^2\ 2\pi^4\ 3\pi^2$. The three states differ only the arrangement of the two electrons in the 3π orbital. The ground state ($X^3\Sigma^-$) has an equilibrium bond length (R_e) of 1.6107 Å. In the first and second excited states ($a^1\Delta$ and $b^1\Sigma^+$), R_e decreases to 1.5783 and 1.5680 Å, respectively.[11] The two excited states lie 9275 cm^{-1} (1.15 eV) and 14 986 cm^{-1} (1.86 eV) above the ground state.

Unlike NCl, there have been very few studies of $(NCl)_2$ (or N_2Cl_2). No experimental information concerning this system (neither the ground state nor any excited states) has been found. One recent theoretical study has characterized the cis and trans isomers of dichlorodiazene (see Figure 1) with the BP86 density functional.[12] Both species are closed shell singlets belonging to the totally symmetric irreducible representations of the C_{2v} and C_{2h} point groups. Geometry optimizations carried out with the BP86 functional and the 6-311+G(3df) basis set yield very short NN bond lengths, R(NN), of 1.240 and 1.219 Å and very long NCl bond lengths, R(NCl), of 1.831 and 1.808 Å for *cis*- and *trans*-dichlorodiazene, respectively. As expected, the NNCl bond angles, θ(NNCl), of the cis isomer (123.0°) are much larger

† Part of the special issue "Donald Setser Festschrift".
‡ University of Mississippi.
§ Emory University.

10.1021/jp025692n CCC: $22.00 © 2002 American Chemical Society
Published on Web 06/18/2002

TABLE 1: Correlation of States for the Interaction of Two NCl Molecules in the X, a, and b States[a]

surface	$C_{\infty v}(D_{\infty h})$ linear	D_{2h} linear	C_{2v} linear	C_{2v} cis	C_{2h} trans	C_2 propeller	C_s planar
			$b^1\Sigma^+ + b^1\Sigma^+$ Manifold (Asymptote = 3.72 eV)				
S_9	$^1\Sigma_{(g)}^+$	^1A_g	$^1A_1$	$^1A_1$	^1A_g	^1A	$^1A'$
			$a^1\Delta + b^1\Sigma^+$ Manifold (Asymptote = 3.01 eV)				
S_8	$^1\Delta_{(g)}(2)$	^1A_g	$^1A_1$	$^1A_1$	^1A_g	^1A	$^1A'$
S_7	$^1\Delta_{(g)}(1)$	$^1B_{1g}$	$^1A_2$	$^1B_1$	^1A_u	^1B	$^1A''$
S_6	$^1\Delta_{(u)}(2)$	^1A_u	$^1A_1$	$^1A_2$	^1B_g	^1A	$^1A''$
S_5	$^1\Delta_{(u)}(1)$	$^1B_{1u}$	$^1A_2$	$^1B_2$	^1B_u	^1B	$^1A'$
			$a^1\Delta + a^1\Delta$ Manifold (Asymptote = 2.30 eV)				
S_4	$^1\Gamma_{(g)}(2)$	^1A_g	$^1A_1$	$^1A_1$	^1A_g	^1A	$^1A'$
S_3	$^1\Gamma_{(g)}(1)$	$^1B_{1g}$	$^1A_2$	$^1B_1$	^1A_u	^1B	$^1A''$
S_2	$^1\Sigma_{(u)}^-$	^1A_u	$^1A_1$	$^1A_1$	^1A_g	^1A	$^1A'$
S_1	$^1\Sigma_{(g)}^+$	^1A_g	$^1A_2$	$^1A_2$	^1B_g	^1A	$^1A''$
			$X^3\Sigma^- + b^1\Sigma^+$ Manifold (Asymptote = 1.86 eV)				
T_7	$^3\Sigma_{(u)}^-$	^3A_u	$^3A_2$	$^3B_1$	^3A_u	^3B	$^3A''$
T_6	$^3\Sigma_{(g)}^-$	$^3B_{1g}$	$^3A_2$	$^3A_2$	^3B_g	^3A	$^3A''$
			$X^3\Sigma^- + a^1\Delta$ Manifold (Asymptote = 1.15 eV)				
T_5	$^3\Delta_{(g)}(2)$	^3A_g	$^3A_1$	$^3A_1$	^3A_g	^3A	$^3A'$
T_4	$^3\Delta_{(g)}(1)$	$^3B_{1g}$	$^3A_2$	$^3B_1$	^3A_u	^3B	$^3A''$
T_3	$^3\Delta_{(u)}(2)$	^3A_u	$^3A_1$	$^3A_2$	^3B_g	^3A	$^3A''$
T_2	$^3\Delta_{(u)}(1)$	$^3B_{1u}$	$^3A_2$	$^3B_2$	^3B_u	^3B	$^3A'$
			$X^3\Sigma^- + X^3\Sigma^-$ Manifold (Asymptote = 0.00 eV)				
Q_1	$^5\Sigma_{(g)}^+$	^5A_g	$^5A_1$	$^5A_1$	^5A_g	^5A	$^5A'$
T_1	$^3\Sigma_{(u)}^+$	$^3B_{1u}$	$^3A_1$	$^3B_2$	^3B_u	^3B	$^3A'$
S_0	$^1\Sigma_{(g)}^+$	^1A_g	$^1A_1$	$^1A_1$	^1A_g	^1A	$^1A'$

[a] The energy of two infinitely separated NCl molecules (i.e., the asymptotic limit) is given in eV for each manifold. The ordering is loosely based on the cis energies near $R(NN) = 2.5$ Å.

than those for the trans structure (108.2°). At this level of theory, the cis isomer is more stable by 6.8 kcal mol^{-1}.

As indicated by eqs 3−5, the ground ($X^3\Sigma^-$) and first two excited states ($a^1\Delta$ and $b^1\Sigma^+$) of NCl must be considered when studying the self-quenching of NCl($a^1\Delta$). Taking into account only these three states of NCl, the interaction of two NCl molecules yields a complicated spectrum of 18 electronic surfaces for $(NCl)_2$. The 18 states are listed in Table 1 and fall into 3! = 6 groups or manifolds corresponding to the different combinations of two NCl molecules (X + X, X + a, X + b, a + a, a + b, and b + b). Each manifold contains all states of $(NCl)_2$ correlating with a particular combination of two NCl molecules at infinite separation. The individual surfaces of each manifold are identified by their multiplicities and (approximate) relative energies. The 10 singlet surfaces are denoted by S_0, S_1, ..., S_9 where S_0 is the ground state and S_9 is the highest lying singlet state under consideration. Similarly, T_1, ..., T_7 are used to label the seven triplet surfaces while Q_1 denotes the lone quintet surface from the X + X manifold.

The asymptotic behavior (i.e., infinite separation of two NCl molecules) of each manifold can be determined from the energies of first and second excited states of NCl[11] (vide supra). The X + a and X + b asymptotes lie 9275 cm^{-1} (1.15 eV) and 14 986 cm^{-1} (1.86 eV) above the X + X asymptote. Simple addition provides the analogous energies for the a + a, a + b, and b + b manifolds: 18 550 cm^{-1} (2.30 eV), 24 261 cm^{-1} (3.01 eV), and 29 972 cm^{-1} (3.72 eV), respectively.

In this study of the self-annihilation of NCl($a^1\Delta$), focus is obviously placed on the a + a manifold. In particular, low-energy, adiabatic pathways from the states of this manifold to the products shown in eqs 3−5 are sought. To obtain some qualitative insight into these possible pathways, this initial study follows the energy of all 18 states listed in Table 1 as two NCl molecules approach each other in high-symmetry nuclear arrangements (e.g., linear, C_{2v} and C_{2h}). Promising candidates are then examined more carefully. Particular attention is paid to the shape of the lowest two singlet states on the a + a manifold (S_1 and S_2) and their interaction with the highest triplet state from the X + b manifold (T_7).

Theoretical Methods

We have employed the state-averaged complete active space self-consistent field (SA-CASSCF) method[13,14] for all calculations in this work. Initially, the SA-CASSCF procedure included all 18 states associated with the interaction of two NCl($X^3\Sigma^-$, $a^1\Delta$, $b^1\Sigma^+$) molecules in the state averaging procedure and employed the full valence (FV) active space corresponding to the Cl 3*s*, N 2*s*, σ, π,π*, and σ* orbitals of NCl. As details of the surfaces were uncovered, it was discovered that these extremely time-consuming calculations could be avoided in certain regions of potential energy surfaces (PESs) by averaging fewer states and utilizing a reduced active space.

Overall, three sets of states were included in the state averaging procedure during this study: (i) all 18 states listed in Table 1, (ii) the 13 states remaining after the 5 high-lying states from the a + b and b + b manifolds are excluded, and (iii) only the 6 states associated with the X + b and a + a manifolds. Two active spaces were employed: (i) the 24 electron/16 orbital (24e/16o) FV active space already defined and (ii) a reduced 16e/12o space which excludes the Cl 3s-like and N 2s-like orbitals. All occupied orbitals not included in the active space were optimized but constrained to be doubly occupied during the CASSCF procedure. Two relatively small basis sets, 6-31+G(d) and 6-311+G(d), were utilized. Five spherical harmonic Gaussian functions were used for the d-atomic orbitals rather than six Cartesian Gaussian functions.

All geometry optimizations were carried out using the analytical gradients[15] available for the SA-CASSCF method in the MOLPRO 2000.1 quantum chemistry program package.[16] Special optimizations to locate mimina on the seams of crossing (MSXs) between electronic states of different spin and/or spatial symmetry were performed with the SEAM program.[17,18] The SEAM program takes gradients computed by MOLPRO for two different states and projects them onto the seam of crossing in order to locate minima on that seam. For states of different symmetry, the procedure is essentially a geometry optimization in $3N - 7$ dimensions due to the additional constraint that the point must lie on the seam of crossing. For all structures reported here, residual gradients (or projections thereof onto the seam of crossing) were less than $1 \times 10^{-4} E_h$/au or E_h/degree.

The MSXs located are on seams between singlet and triplet surfaces. Although spin-forbidden, a transition between the two surfaces can occur due to spin−orbit interactions. The spin−orbit matrix element between the two states associated with the seam was computed at each MSX by the full Breit−Pauli spin−orbit Hamiltonian.

With the larger FV active space, SA-CASSCF geometry optimizations proved to be prohibitively expensive. In C_{2v} symmetry, a single SA-CASSCF gradient for the smallest set of states (6) required nearly 48 h on a single CPU of an IBM SP2 with a 375 MHz Power3 processor and used nearly 2 GB of RAM as well as 18 GB of disk space. Since MSX optimizations require two gradients per cycle (one for each surface), it was possible to locate MSXs in a reasonable amount of time only with the smaller active space (approximately 6 h per SA-CASSCF gradient).

It is important to note, however, that the reduced 16e/12o active space is not applicable to all regions of the PESs. In

TABLE 2: Bond Lengths (Å) and Energies of the Ground ($X^3\Sigma^-$) and First Two Excited ($a^1\Delta$ and $b^1\Sigma^+$) States of NCl[a]

CASSCF	basis	*R*(NCl)(*X*)	*R*(NCl)(a)	*R*(NCl)(b)	*E*(X)	$E_{relative}$(a)	$E_{relative}$(b)
			Averaging a and b States				
16e/12o	6-31+G(d)	1.694	1.645	1.622	−513.82156	1.42	2.55
16e/12o	6-311+G(d)	1.695	1.645	1.622	−513.86024	1.42	2.55
24e/16o	6-31+G(d)	1.698	1.650	1.642	−513.82488	1.48	2.10
24e/16o	6-311+G(d)	1.698	1.650	1.642	−513.86361	1.48	2.10
			Averaging X, a, and b States				
16e/12o	6-31+G(d)	1.697	1.645	1.620	−513.82176	1.47	2.63
16e/12o	6-311+G(d)	1.697	1.645	1.620	−513.86045	1.47	2.64
24e/16o	6-31+G(d)	1.698	1.650	1.641	−513.82487	1.52	2.16
24e/16o	6-31+G(d)	1.699	1.650	1.641	−513.86359	1.52	2.16
experiment[b]		1.6107	1.5783	1.5680		1.15	1.86

[a] The total energy of the ground state is in E_h while the relative energies of the excited states are given in eV. The 24 electron/16 orbital (24e/16o) active space corresponds to the full-valence space. [b] Reference 11.

particular, the 16e/12o active space is problematic for ClN···NCl separations near 2.0 Å. At this point the electronic structure begins to change dramatically in anticipation of what could be considered the formation of an NN double bond in light of the computational study of the ground state of dihalodiazenes.[12] The N 2s-like orbitals move into the valence region, while several of the 3p-like orbitals on the Cl atoms move out of the valence space as their nature changes from σ and π bond character to that of lone-pair orbitals. While it will almost certainly be possible to select another truncated space at shorter intermolecular separations, it appears that FV-CASSCF computations are in order for this sensitive region of the PES.

Results and Discussion

NCl ($X^3\Sigma^-$, $a^1\Delta$, $b^1\Sigma^+$). A summary of the bond lengths and energies of the three lowest lying states of NCl have been collected in Table 2. The SA-CASSCF procedure provides qualitative agreement with experiment. However, bond lengths are too long and excited states too high. Both basis sets yield nearly identical results for the relative energies and bond lengths. However, the two active spaces predict rather different values for the energy and bond length of the second excited state ($b^1\Sigma^+$). The larger FV active space (24e12o) reproduces the experimentally observed spacing between the a and b states (1.86 − 1.15 = 0.71 eV) much better than the 16e/12o reduced active space. Unfortunately, computations using the FV active space are prohibitively expensive for two NCl molecules except for occasional energy points.

Collinear Scans of the NCl + NCl System. Three linear nuclear configurations have been considered: NCl···ClN, NCl···NCl, and ClN···NCl. For these high symmetry structures, all 18 electronic surfaces were scanned. Although only 13 states can be seen in Figure 2, five states ($^1\Delta_{(g)}$ and $^1\Delta_{(u)}$ from the a + b manifold, $^1\Gamma_{(g)}$ from the a + a manifold, and $^3\Delta_{(g)}$ and $^3\Delta_{(u)}$ from the X + a manifold) are doubly degenerate for these linear arrangements.

Rigid scans were performed as the two NCl molecules approach each other. The NCl bond lengths were fixed at 1.59 Å (about halfway between the experimental bond lengths for the ground and excited states of NCl). All surfaces are highly repulsive. When the collinear NCl units are less than 2.5 or 3.0 Å apart, the energy of each state rises rapidly. Not surprisingly, the surfaces are most repulsive when the Cl atoms are oriented toward each other (NCl···ClN) as in Figure 2a. Rotating one of the NCl units by 180° (NCl···NCl) decreases the rate at which the energies increase as separation decreases (Figure 2b). With the two N atoms pointing toward each other (ClN···NCl), most surfaces are slightly flatter but have the same overall behavior (Figure 2c).

A few important features of the NCl + NCl PESs can immediately be extracted from these collinear scans. (i) The energies of the highest two manifolds (b + b and a + b) do not come close to those of the a + a manifold except at extremely high energies (more than 1 or 2 eV above the a + a asymptote). (ii) Likewise, the lowest two manifolds (X + X and X + a) are well separated from the a + a manifold. The corresponding states do not interact with the a + a manifold except when the intermolecular separation is small. (iii) The X + b manifold is nearly resonant with the a + a manifold. Only states from the X + b manifold appear to be candidates for long-range, low-energy interactions with the a + a manifold. At this point, the computational procedure was simplified tremendously by excluding the five states from the high-lying a + b and b + b manifolds from all subsequent calculations.

***C_{2v}* and *C_{2h}* Scans of the NCl + NCl System.** The work of Nordhoff and Anders on *cis*- and *trans*-dihalodiazenes[12] suggests that C_{2v} and C_{2h} arrangements of the two NCl fragments could be better candidates than collinear structures. Scans of NCl + NCl configurations that mimic the structure of cis- and *trans*-dichlorodiazene (shown in Figure 1) were carried out in C_{2v} and C_{2h} point group symmetry, respectively. For these rigid scans, *R*(NCl) was fixed at 1.645 Å and θ(NNCl) 120.0°. The qualitative differences between these cis and trans scans and the collinear ones are immediately apparent.

As can be seen in Figure 3, the triplet (T_1) and quintet (Q_1) surfaces in the X + X manifold are still quite repulsive. An interesting new feature of this manifold can be seen for small *R*(NN) where the ground-state singlet surface (S_0) actually begins to exhibit an attractive potential. This attractive region on S_0 corresponds to the formation of the double bond in *cis*- and *trans*-dichlorodiazene. However, high level computations on S_0 that will be presented elsewhere question the stability of these dichlorodiazene isomers with respect to dissociation into N_2 and two Cl atoms or into NNCl and one Cl atom.[19]

The surfaces in the X + a manifold are still rather repulsive. However, the energy of T_2 does not increase nearly as quickly as the other three states and may actually become attractive at shorter NN distances. Unfortunately, that region of the PES cannot be explored with the 16e/12o active space that we have employed thus far. The formation of the NN double bond mentioned in the previous paragraph drastically alters the occupation, the energy, and therefore the ordering of the orbitals. Recall that the 16e/12o active space includes all valence orbitals *except* the Cl 3*s*-like and N 2*s*-like orbitals. At the dichlorodiazene geometries reported by Nordhoff and Anders,[12] the N 2*s*-like orbitals have occupations and energies similar to the newly formed NN σ bond and should not be excluded from the active space.

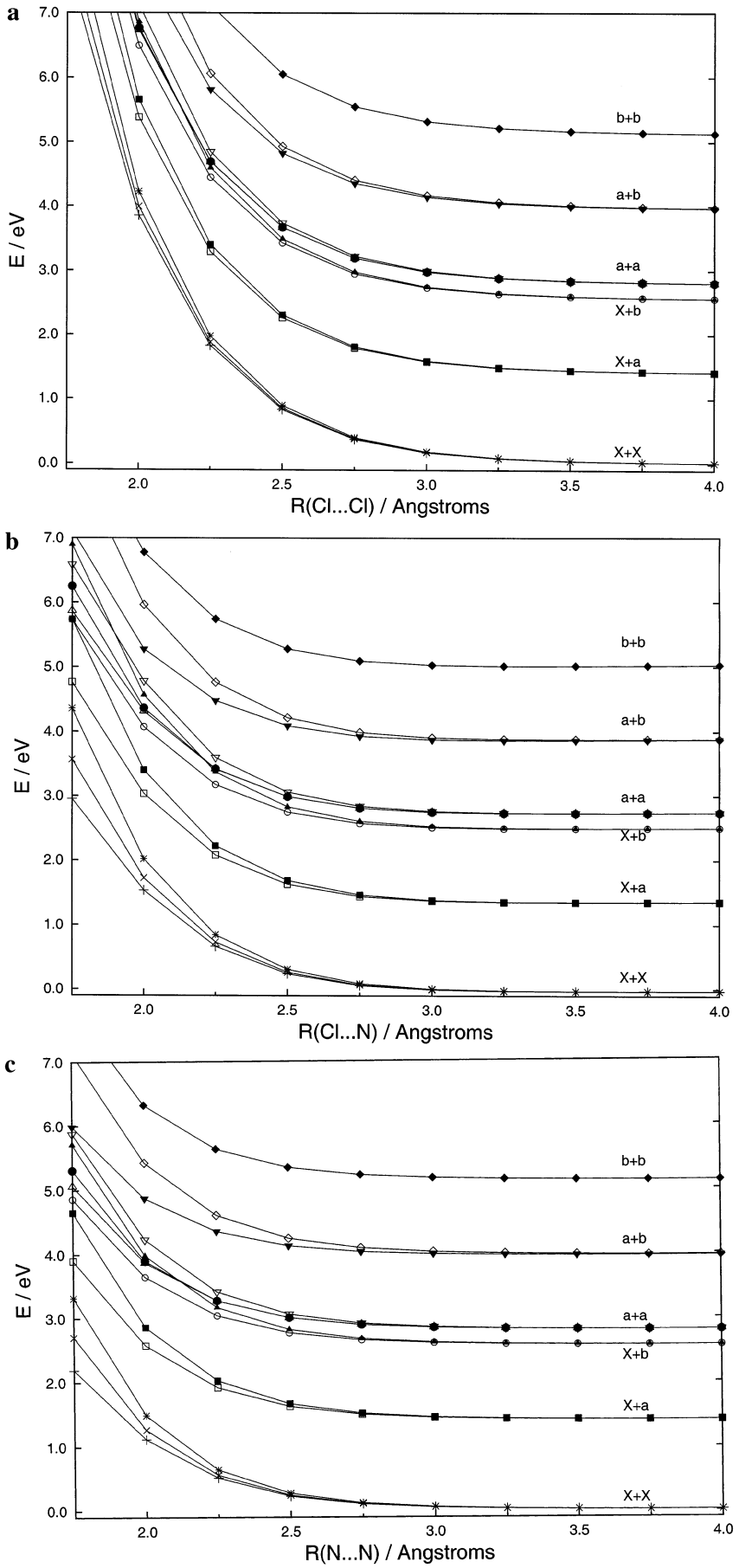

Figure 2. Rigid SA-CASSCF scans of the collinear configurations of the NCl + NCl system. The energies (eV) are relative to two infinitely separated NCl($X^3\Sigma^-$) molecules. For all calculations the 16e/12o active space and 6-31+G(d) basis set were used. *R*(NCl) was set to 1.59 Å. (a) Colinear NCl...ClN scan. (b) Colinear NCl...NCl scan. (c) Colinear ClN...NCl scan.

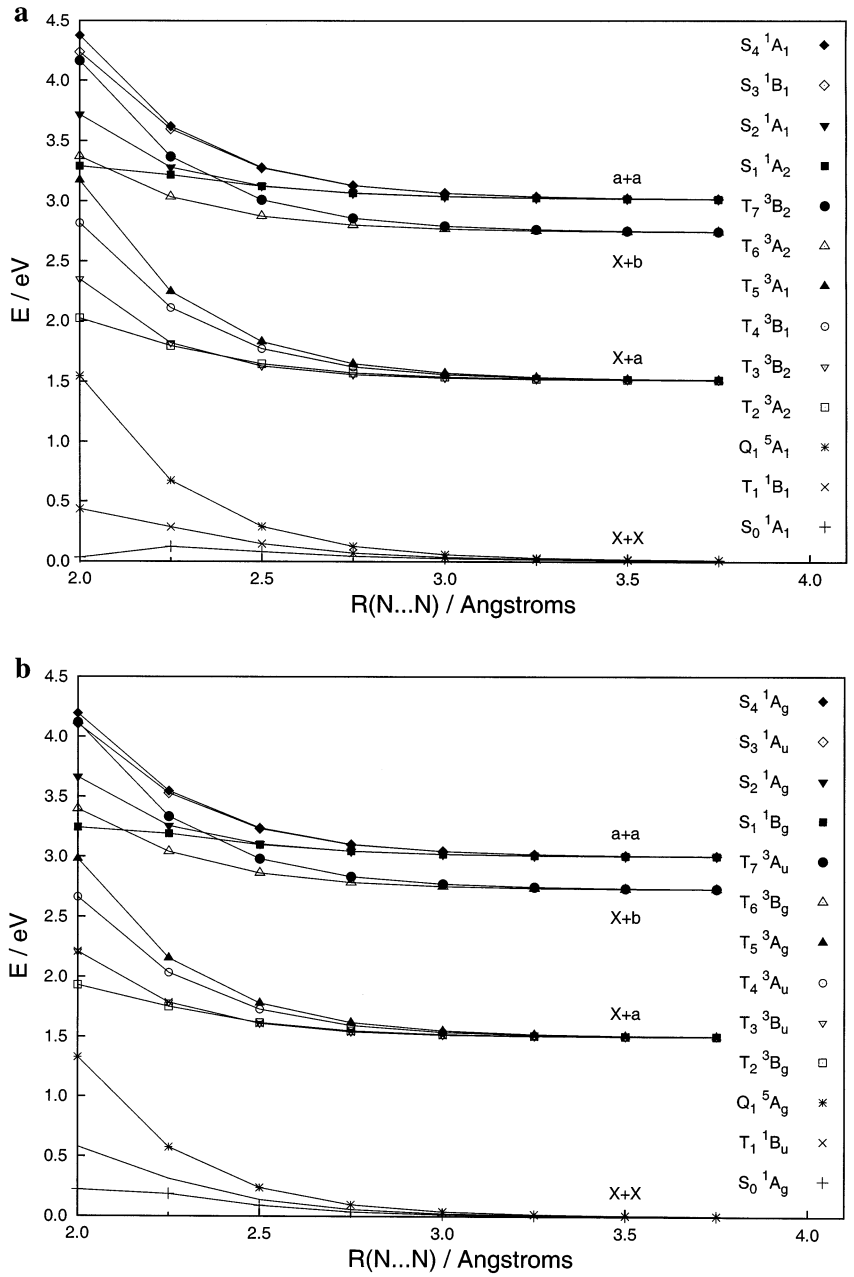

Figure 3. Rigid SA-CASSCF scans of the cis and trans configurations of the NCl + NCl system. The energies (eV) are relative to two infinitely separated NCl($X^3\Sigma^-$) molecules. For all calculations the 16e/12o active space and 6-311+G(d) basis set were used. R(NCl) was set to 1.645 Å and θ(NNCl) to 120.0°. (a) C_{2v} scan of the NCl + NCl system. (b) C_{2h} scan of the NCl + NCl system.

Careful inspection of the a + a and X + b manifolds reveals more interesting behavior. While S_3 and S_4 are still quite repulsive and quickly rise in energy as the NCl molecules approach each other, the energy associated with S_1 and S_2 does not increase significantly until R(NN) is less than 2.25 Å. S_1, in fact, remains very flat throughout the entire scan. At the same time, T_7 rises very quickly and crosses both S_1 and S_2 at very low energies (a small fraction of an electronvolt) relative to the a + a dissociation asymptote. These crossings occurs at roughly R(NN) = 2.4 Å for both the cis and trans orientations.

Since X + b is the only manifold to interact significantly with the a + a manifold, only the six states (T_6, T_7, S_1, S_2, S_3, S_4) belonging to these manifolds are included in the state averaging procedure for the remaining calculations unless otherwise noted. In addition, the energy of seven states from the lower two manifolds are computed only if they are of the same spin and spatial symmetry as T_6, T_7, S_1, S_2, S_3, or S_4.

It should be noted that Figure 3 shows additional low-energy crossings. Near 2.1 Å, S_1 and T_6 cross. It also appears that S_1 will cross T_5 from the X + a channel in the region where R(NN) = 1.9 Å. However, these 4 additional crossings occur in regions of the PESs currently beyond our capabilities to characterize (see Conclusions and Outlook).

High-Symmetry MSXs. Having identified 8 low-energy crossings that correspond to the quenching pathway in eq 3, seam optimizations were carried out in C_{2v} and C_{2h} symmetry to find the mimina on the seams of crossing (MSXs). These optimization were only possible for 4 the crossings that occur near R(NN) = 2.4 Å (see Conclusions and Outlook). In this region, the T_7 surface from the X + b manifold crosses both the S_1 and S_2 surfaces from the a + a manifold. These seams are denoted as T_7/S_1 and T_7/S_2. The prefix cis and trans are added to indicate the orientation since the crossings occur in both C_{2v} and C_{2h} symmetry.

TABLE 3: C_{2v} and C_{2h} Structures of the Minima on the Seams of Crossing between the T_7 Surface from the X + b Manifold and the S_1 and S_2 Surfaces from the a + a Manifold[a]

CAS	basis	R(NN)	R(NCl)	θ(NNCl)	$E_{relative}$	$\lvert\langle S\rvert\mathscr{H}^{SO}\lvert T\rangle\rvert$/ cm^{-1} i
		Cis T_7/S_1 (C_{2v} Point Group)				
16e/12o	6-31+G(d)	2.387	1.654	114.5	+3.4	1.91
16e/12o	6-311+G(d)	2.385	1.654	114.6	+3.2	1.90
		Cis T_7/S_2 (C_{2v} Point Group)				
16e/12o	6-31+G(d)	2.364	1.651	114.1	+4.3	13.62
16e/12o	6-311+G(d)	2.361	1.651	114.4	+4.5	14.90
		Trans T_7/S_1 (C_{2h} Point Group)				
16e/12o	6-31+G(d)	2.384	1.646	108.5	+2.1	0.0
16e/12o	6-311+G(d)	2.384	1.646	108.6	+1.8	0.0
		Trans T_7/S_2 (C_{2h} Point Group)				
16e/12o	6-31+G(d)	2.354	1.643	108.7	+3.1	0.0
16e/12o	6-311+G(d)	2.354	1.643	108.6	+2.8	0.0

[a] Bond lengths are in Ångstroms and bond angles in degrees. The energy relative to the a + a asymptote (i.e., two infinitely separated NCl(a$^1\Delta$) molecules) is given in kcal mol^{-1}. The last column gives the spin−orbit matrix elements (in cm^{-1} i) for the full Breit−Pauli operator.

A summary of the structure corresponding to the 4 optimized MSXs is presented in Table 3. Both the cis and trans T_7/S_1 MSXs occur near R(NN) = 2.38 Å, while the T_7/S_1 minima are near R(NN) = 2.36 Å. With the exception of this long NN distance, the structures of the cis and trans MSXs are very similar to the dichlorodiazene isomers (see Figure 1 and text in Introduction). All 4 MSXs appear to be energetically accessible. At the theoretical levels employed here, they lie just a few kcal mol^{-1} above the a + a asymptote. While a transition from S_1 or S_2 to T_7 may be energetically accessible, it is a spin forbidden process. However, transition between the singlet and triplet states takes place through the spin−orbit interaction with its probability proportional to the square of the absolute value of the spin−orbit matrix element. The spin−orbit matrix element $\mathscr{H}_{SO}$ associated with this process at each MSX was determined with the spin−orbit code available in MOLPRO. The results are included in Table 3.

Again, we emphasize that there should be 4 more low-energy MSXs at shorter NN distances (R(NN) ≈ 2.0 Å). Using the notation introduced in this section they are denoted cis T_6/S_1, trans T_6/S_1, cis T_5/S_1, and trans T_5/S_1. The corresponding MSXs could not be characterized since the 16e/12o active space breaks down inside 2.2 Å, and FV 24e/16o gradients were too expensive computationally.

***C_2* Scans Near MSXs.** As noted above, the four low-energy MSXs listed in Table 3 were found during seam optimization that were constrained to C_{2v} and C_{2h} symmetry. Lower symmetry cases must be considered because, unlike normal geometry optimizations, lowering the symmetry in a MSX optimization does not guarantee that the energy will decrease (or stay the same). Unfortunately, gradient calculations in C_s and C_2 symmetry are quite time-consuming, to say nothing of C_1 symmetry. As a compromise, we first performed a series of rigid torsional scans near the MSXs to determine whether the NCl(a) + NCl(a) complex prefers to be planar. For the scans near the cis MSXs, the NCl bond lengths and NNCl bond angles were fixed at values similar to those of the optimized MSXs (R(NCl) = 1.6525 Å and θ(NNCl) = 114.45°). Likewise, R(NCl) was set to 1.644 Å and θ(NNCl) to 108.5° for the trans MSX region.

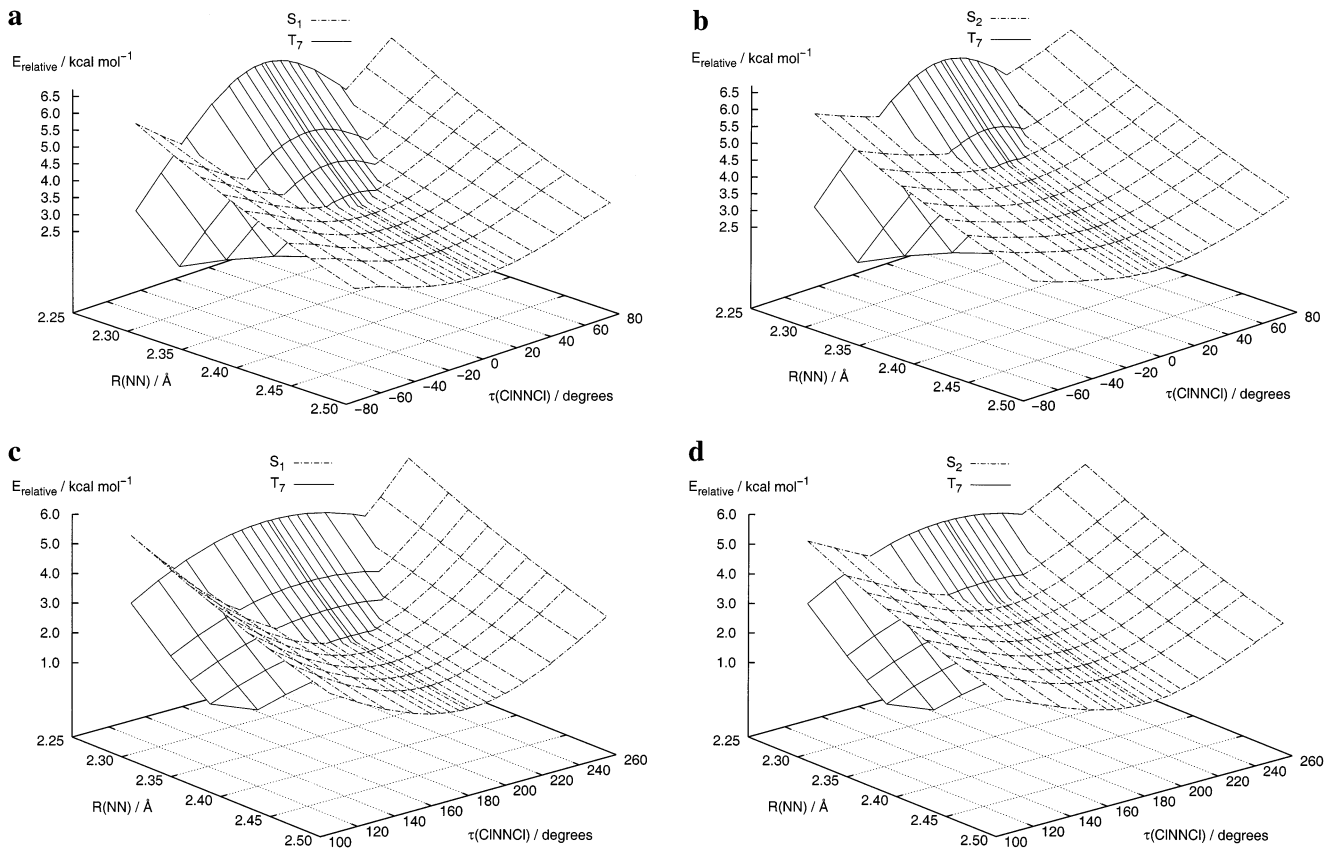

Figure 4. Rigid SA-CASSCF C_2 scans near the four cis and trans MSXs. The energies (kcal mol^{-1}) are relative to two infinitely separated NCl(a$^1\Delta$) molecules. For all calculations the 16e/12o active space and 6-31+G(d) basis set were used. R(NCl) was set to 1.6525 Å and θ(NNCl) to 114.45° for the scans near the cis MSXs, while these geometrical parameters were constrained to R(NCl) = 1.644 Å, θ(NNCl) = 108.5° for the trans MSX region. (a) C_2 scan near the cis T_7/S_1 MSX. (b) C_2 scan near the cis T_7/S_2 MSX. (c) C_2 scan near the trans T_7/S_1 MSX. (d) C_2 scan near the trans T_7/S_2 MSX.

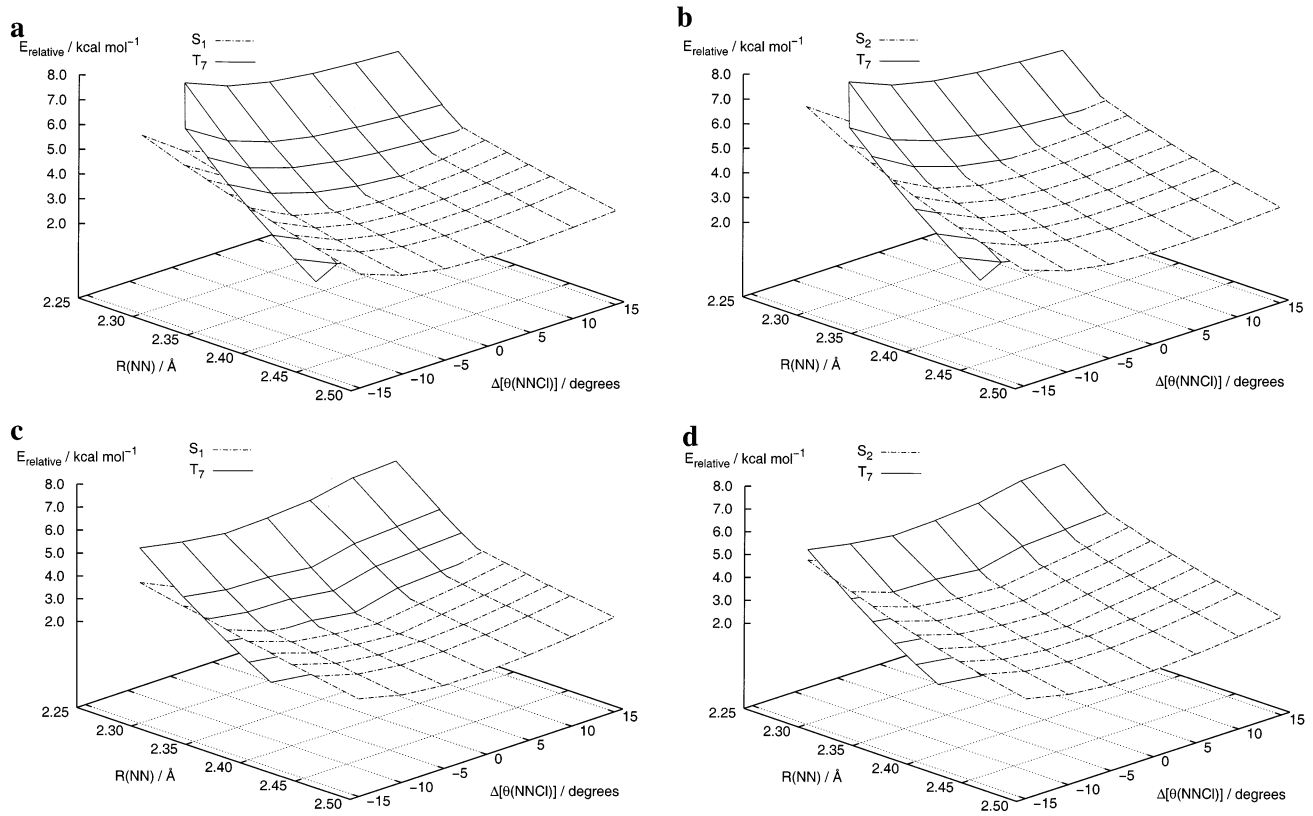

Figure 5. Rigid SA-CASSCF C_s scans near the four cis and trans MSXs. The energies (kcal mol^{-1}) are relative to two infinitely separated NCl($a^1\Delta$) molecules. For all calculations the 16e/12o active space and 6-31+G(d) basis set were used. Both R(NCl) distances were set to 1.6525 Å for the scans near the cis MSXs and to 1.644 Å for the trans MSX region. One θ(NNCl) bond angle was fixed (114.45° for the cis MSX and 108.5° for the trans MSX), while the other bond angle was varied. The difference between the two angles, $\Delta[\theta(\text{NNCl})]$, is the angular coordinate used here. (a) C_s scan near the cis T_7/S_1 MSX. (b) C_s scan near the cis T_7/S_2 MSX. (c) C_s scan near the trans T_7/S_1 MSX. (d) C_s scan near the trans T_7/S_2 MSX.

For all four crossings, the singlet and triplet surfaces have been plotted in Figure 4 for various torsional angles, τ(ClNNCl), and NN distances, R(NN). The C_2 minimum energy pathway for the singlet surfaces (S_1 and S_2) occurs at 0° for the cis arrangement and 180° for the trans orientation. T_7, on the other hand, has very pronounced negative curvature in this region and actually reaches maxima at torsional angles of 0° and 180°. As can be seen in Figure 4, this topological combination places the minimum on the seam of crossing at either 0° or 180° for the cis and trans configuratoins. This result suggests the MSXs are indeed planar.

It is clear that at NN distances larger than or near the MSXs, there is very little barrier to rotation between cis and trans configurations on the singlet surfaces. Although not shown here, for R(NN) > 3.5 Å, this barrier on S_1 is essentially nonexistent. In fact, the S_1 and S_2 potentials are so flat in this region that optimizations of the torsional angle for fixed R(NN) are extremely problematic.

***C_s* Scans Near MSXs.** Next, a series of C_s scans were performed in a fashion similar to those in the previous section. For these planar nuclear configurations, both NCl bonds, R(NCl), were fixed at the same values used above (1.6525 Å for cis-like and 1.644 Å for trans-like structure), but just one of the NNCl angles, θ(NNCl), was fixed (114.45° and 108.5°, respectively). The other NNCl angle was varied, and the difference between the two angles, $\Delta[\theta(\text{NNCl})]$, is the angular coordinate used in Figure 5. Thus, these planar structures belong to the C_{2v} or C_{2h} point group when $\Delta[\theta(\text{NNCl})]$ is equal to zero (since the two NCl bond lengths are equal).

The surfaces associated with each of the four seams of crossing have been plotted in Figure 5 for various values of R(NN) and $\Delta[\theta(\text{NNCl})]$. One glaring difference between these C_s scans and the C_2 scans of section 3.5 is the curvature of T_7, which is positive along the $\Delta[\theta(\text{NNCl})]$ coordinate but negative along τ(ClNNCl). The surfaces are again quite flat, but the small region scanned (±15°) could be misleading in this respect. For larger negative values of $\Delta[\theta(\text{NNCl})]$, the potential should rise very quickly as the Cl atom of one NCl unit approaches the N atom of the other NCl molecule. When $\Delta[\theta(\text{NNCl})] = -\theta(\text{NNCl})$, the molecules are colinear, and the distance between these two atoms is only R(NN) − R(NCl).

Determining the C_s minimum energy pathway for these surfaces is a bit more difficult than for the C_2 case since they are no longer symmetric about the angular coordinate. Nevertheless, the point of lowest energy on the seam connecting the singlet and triplet surfaces is not located at $\Delta[\theta(\text{NNCl})] = 0°$ (i.e., configurations with both NNCl angles equal). The minimum appears to be located between $\Delta[\theta(\text{NNCl})] = -5$ and −10°, which implies the NCl($a^1\Delta$) + NCl($a^1\Delta$) system prefers a C_s structure that is slightly distorted from the C_{2v} cis and C_{2h} trans configurations.

Conclusions and Outlook

In a search for potential long-range, low-energy self-annihilation pathways of NCl($a^1\Delta$), we have carried out numerous scans of the lowest 18 electronic surfaces that correlate with the interaction of two NCl molecules in the $X^3\Sigma^-$, $a^1\Delta$, and $b^1\Sigma^+$ states. For intermolecular separations greater than 2.2 Å, only the T_7 triplet state from the nearly resonant X + b channel interacts with the states of the a + a manifold. In fact, T_7 crosses both S_1 and S_2 at very low energies relative to the a + a

asymptote. These crossings occur when the two NCl units are in both a cis and trans orientation (analogous to those shown in Figure 1), and the two N atoms are approximately 2.37 Å apart. In C_{2v} and C_{2h} symmetry, the four optimized MSXs (cis T_7/S_1, cis T_7/S_2, trans T_7/S_1 and trans T_7/S_2) are only 1.8−4.5 kcal mol^{-1} above the a + a entrance channel at the theoretical levels employed here. The trans MSXs are located 1−2 kcal mol^{-1} below the cis structures. The T_7/S_1-MSXs also lie about 1 kcal mol^{-1} below the T_7/S_2-MSXs.

At shorter intermolecular separations (R(NN) ≈ 2.0 Å), four other low-energy crossings were identified (cis T_6/S_1, trans T_6/S_1, cis T_5/S_1, and trans T_5/S_1). The corresponding MSXs could not be characterized due to technical problems for R(NN) < 2.2 Å (vide infra). Work is currently underway to address this issue and characterize the short-range region of the PESs.

C_2 torsional scans near the MSXs indicate that the minimum energy a + a entrance channel is indeed planar. The T_7 surface exhibits the opposite curvature and actually reaches maxima at planar configurations. For intermolecular separations above 3.5 Å the barrier to rotation on the S_1 and S_2 surfaces is essentially nonexistent.

Scans of cis- and trans-like planar NCl + NCl arrangements near the MSXs indicate that the minimum energy pathways on the S_1, S_2, and T_7 surfaces are slightly distorted from C_{2v} cis and C_{2h} trans structures to C_s orientations. However, the PESs are quite flat with respect to differences in the two NNCl angles (one measure of the deviation from C_{2v} or C_{2h} symmetry). It is therefore reasonable to expect that the C_s MSXs would only be slightly lower in energy than the high-symmetry ones.

Although this investigation has revealed much about the interaction of two NCl($a^1\Delta$) molecules, there were several important points we did not address due to the excessive computational demands associated with them. One such matter is the characterization of the MSXs in C_s or even C_1 symmetry and at higher levels of theory. This includes concerns about the effects of dynamical correlation on the structure and energies of the MSXs, which can be assessed with methods such as complete active space second-order perturbation theory (CASPT2) and multireference configuration interaction theory (MRCI). Also of interest is the behavior of the PESs at shorter R(NN) distances. In particular, while the S_3 and S_4 surfaces become very repulsive as R(NN) approaches 2.0 Å, the S_1 surface remains quite flat. It is possible that S_1 and perhaps even S_2 become atractive after passing over some barrier. Both the barrier heights to and depths of these attractive regions of the PESs would be very useful if they exist. S_1 and S_2 energy wells could lead to low-energy crossing with states from the X + a and even X + X manifolds. In addition, other low-energy crossings occur near 2.2 Å. Unfortunately, studying the transition from the long-range region of the NCl + NCl PESs (R(NN) > 2.2 Å) to the areas with small values of R(NN) requires a large active space which, like the MRCI and CASPT2 methods, is prohibitively expensive.

This qualitative survey of the PESs associated with the a + a manifold has identified 8 long-range quenching pathways that are energetically accessible at the temperatures at which CAIL systems will operate. It also suggests that short-range interactions may also be important in the self-annihilation of NCl($a^1\Delta$). Additional work is already undeway to address this issue and to extend this work from a qualitative description of these PESs to a quantitative understanding of all three quenching pathways in eqs 3−5. The short-range NCl($a^1\Delta$) + NCl($a^1\Delta$) interactions are being characterized with methods similar to those employed in this work. Once key regions and MSXs of the PESs have been identified from these qualitative studies, the structures and energetics can be characterized more reliably with larger basis sets and methods that recover dynamical electron correlation outside of the active space (e.g., MRCI and CASPT2).

Acknowledgment. We are grateful to Dr. A. L. Kaledin for invaluble technical assistance and suggestions at the early stages of this project. We acknowledge support for this project from the Air Force Office of Scientific Research (AFOSR-F49620-01-1-0183 to K.M.) and the Cherry L. Emerson Center for Scientific Computation, which is in part supported by a National Science Foundation grant (CHE-0079627) and an IBM Shared University Research award. This project was initiated during a postdoctoral stay by G.S.T. at Emory University.

References and Notes

(1) Bower, R. D.; Yang, T. T. *J. Opt. Soc. Am. B: Opt. Phys.* **1991**, *8*, 1583.
(2) Yang, T. T.; Gylys, V. T.; Bower, R. D.; Rubin, L. F. *Opt. Lett.* **1992**, *17*, 1803.
(3) Ray, A. J; Coombe, R. D. *J. Phys. Chem.* **1993**, *97*, 3475.
(4) Ray, A. J.; Coombe, R. D. *J. Phys. Chem.* **1995**, *99*, 7849.
(5) Herbelin, J. M.; Henshaw, T. L.; Rafferty, B. D.; Anderson, B. T.; Tate, R. F.; Madden, T. J.; Manke, G. C. *Chem. Phys. Lett.* **1999**, *299*, 583.
(6) Henshaw, T. L.; Herrera, S. D.; Haggquist, G. W.; Schlie, L. A. *J. Phys. Chem. A* **1997**, *101*, 4048.
(7) Henshaw, T. L.; Manke, G. C.; Madden, T. J.; Berman, M. R.; Hager, G. D. *Chem. Phys. Lett.* **2000**, *325*, 537.
(8) Manke, G. C.; Setser, D. W. *J. Phys. Chem. A* **1998**, *102*, 153.
(9) Manke, G. C.; Setser, D. W. *J. Phys. Chem. A* **1998**, *102*, 7257.
(10) Hewett, K. B.; Manke, G. C.; Setser, D. W.; Brewood, G. *J. Phys. Chem. A* **2000**, *104*, 539.
(11) Huber, K. P.; Herzberg, G. *Constants of Diatomic Molecules*; Van Nostrand Reinhold: New York, 1979.
(12) Nordhoff, K.; Anders, E. *J. Org. Chem.* **1999**, *64*, 7485.
(13) Werner, H.-J.; Knowles, P. J. *J. Chem. Phys.* **1985**, *82*, 5053.
(14) Knowles, P. J.; Werner, H.-J. *Chem. Phys. Lett.* **1985**, *115*, 259.
(15) Busch, T.; Degli Esposti, A.; Werner, H.-J. *J. Chem. Phys.* **1991**, *94*, 6708.
(16) Amos, R. D.; Bernhardsson, A.; Berning, A.; Celani, P.; Cooper, D. L.; Deegan, M. J. O.; Dobbyn, A. J.; Eckert, F.; Hampel, C.; Hetzer, G.; et al. *Molpro, a package of ab initio programs designed by H.-J. Werner and P. J. Knowles*, version 2002.1, 2002.
(17) Dunn, K.; Morokuma, K. *J. Chem. Phys.* **1995**, *102*, 4904.
(18) Cui, Q.; Morokuma, K.; Stanton, J. F. *Chem. Phys. Lett.* **1996**, *263*, 46.
(19) Tschumper, G. S. Work in progress.